Multimodal imaging of choroidal lesions in disseminated mycobacterium chimaera infection after cardiothoracic surgery

Böni, Christian ; Al-Sheikh, Mayss ; Hasse, Barbara ; Eberhard, Roman ; Kohler, Philipp ; Hasler, Pascal W ; Erb, Stefan ; Hoffmann, Matthias ; Barthelmes, Daniel ; Zweifel, Sandrine A

Abstract: PURPOSE: To explore morphologic characteristics of choroidal lesions in patients with disseminated Mycobacterium chimaera infection subsequent to open-heart surgery. METHODS: Nine patients (18 eyes) with systemic M. chimaera infection were reviewed. Activity of choroidal lesions were evaluated using biomicroscopy, fundus autofluorescence, enhanced depth imaging optical coherence tomography, fluorescein angiography/indocyanine green angiography, and optical coherence tomography angiography. Relationships of choroidal findings to systemic disease activity were sought. RESULTS: All 9 male patients, aged between 49 and 66 years, were diagnosed with endocarditis and/or aortic graft infection. Mean follow-up was 17.6 months. Four patients had only inactive lesions (mild disease). In all five patients (10 eyes) with progressive ocular disease, indocyanine green angiography was superior to other tests for revealing new lesions and active lesions correlated with hyporeflective choroidal areas on enhanced depth imaging optical coherence tomography. One eye with a large choroidal granuloma developed choroidal neovascularization. Optical coherence tomography angiography showed areas with reduced perfusion at the inner choroid. All 5 patients with progressive ocular disease had evidence of systemic disease activity within ±6 weeks' duration. CONCLUSION: Choroidal manifestation of disseminated M. chimaera infection indicates systemic disease activity. Multimodal imaging is suitable to recognize progressive ocular disease. We propose ophthalmologic screening examinations for patients with M. chimaera infection.

DOI: https://doi.org/10.1097/IAE.0000000000001991

MULTIMODAL IMAGING OF CHOROIDAL LESIONS IN DISSEMINATED *MYCOBACTERIUM CHIMAERA* INFECTION AFTER CARDIOTHORACIC SURGERY

CHRISTIAN BÖNI, MD,* MAYSS AL-SHEIKH, MD,* BARBARA HASSE, MD,† ROMAN EBERHARD, MD,* PHILIPP KOHLER, MD, MSc,†‡ PASCAL HASLER, MD,§ STEFAN ERB, MD,¶ MATTHIAS HOFFMANN, MD,‡ DANIEL BARTHELMES, MD, PhD,*** SANDRINE A. ZWEIFEL, MD*

Purpose: To explore morphologic characteristics of choroidal lesions in patients with disseminated *Mycobacterium chimaera* infection subsequent to open-heart surgery.

Methods: Nine patients (18 eyes) with systemic *M. chimaera* infection were reviewed. Activity of choroidal lesions were evaluated using biomicroscopy, fundus autofluorescence, enhanced depth imaging optical coherence tomography, fluorescein angiography/indocyanine green angiography, and optical coherence tomography angiography. Relationships of choroidal findings to systemic disease activity were sought.

Results: All 9 male patients, aged between 49 and 66 years, were diagnosed with endocarditis and/or aortic graft infection. Mean follow-up was 17.6 months. Four patients had only inactive lesions (mild disease). In all five patients (10 eyes) with progressive ocular disease, indocyanine green angiography was superior to other tests for revealing new lesions and active lesions correlated with hyporeflective choroidal areas on enhanced depth imaging optical coherence tomography. One eye with a large choroidal granuloma developed choroidal neovascularization. Optical coherence tomography angiography showed areas with reduced perfusion at the inner choroid. All 5 patients with progressive ocular disease had evidence of systemic disease activity within ±6 weeks' duration.

Conclusion: Choroidal manifestation of disseminated *M. chimaera* infection indicates systemic disease activity. Multimodal imaging is suitable to recognize progressive ocular disease. We propose ophthalmologic screening examinations for patients with *M. chimaera* infection.

RETINA 0:1–13, 2017

Recently, *Mycobacterium chimaera,* a slowly growing nontuberculous mycobacterium, has attracted attention because of a global health care–associated outbreak of invasive infections after cardiothoracic surgery.[1] Currently, over 100 patients from more than 10 countries have been reported to suffer from invasive *M. chimaera* infection.[2–6] These infections resulted from aerosolized *M. chimaera* originating from water tanks of heater cooler units used in cardiovascular surgery with extracorporeal circulation for heating/cooling purposes.[1] Because this disease entity is still relatively unknown, misdiagnosing of clinical signs seems probable and the actual prevalence of *M. chimaera* infection may be substantially higher.[4]

Clinical and histopathological findings of five patients with ocular *M. chimaera* infection have been described recently.[7] All five patients presented with chorioretinal lesions and a subset of patients had additional signs of mild anterior uveitis, intermediate uveitis, or disc swelling. During follow-up, the number of chorioretinal lesions was progressive in three of five patients despite extensive antimicrobial therapy and three of five patients died from complications of disseminated *M. chimaera* infection.

Because of growing relevance of this health care–related infection, we herein aim to characterize choroidal lesions in disseminated *M. chimaera* infection of nine patients through multimodal imaging.

We reviewed differences between active and inactive ocular findings. We also tested the hypothesis that these lesions were related to the systemic affection and sought relationships to systemic disease activity and therapy.

Materials, Subjects, and Methods

Case Detection

Methods of case finding and detection have been described previously.[1,2,7] Briefly, patients had undergone open-heart surgery and have subsequently been diagnosed with *M. chimaera* infection based on either positive mycobacterial tissue cultures, 16SrRNA PCR, or mycobacterial blood cultures. Ocular findings were collected at baseline of *M. chimaera* diagnosis and during prospective follow-up. For the current study, ophthalmologic findings of the patients treated at the University Hospital Zurich were completed, and supplemented by four additional cases of disseminated *M. chimaera* infections with ocular involvement from the University Hospital Basel. Institutional review board approval was obtained and all patients provided informed consent to publish their clinical data.

Clinical Aspects

Patients with disseminated *M. chimaera* infection were initially treated with a 4- or 5-fold tuberculostatic therapy containing clarithromycin, ethambutol, rifabutin, and moxifloxacin ± amikacin with the goal of an early redo surgery with replacement of all cardiac foreign material if possible (Table 1). At the time of redo surgery and during clinical follow-up, blood and tissue cultures for mycobacteria were obtained. Systemic disease activity was defined as new positive blood cultures for mycobacteria and/or new positive mycobacterial cultures from a normally sterile site either while on tuberculostatic therapy (breakthrough infection) or in the posttreatment period (relapse).

From the *Department of Ophthalmology, University Hospital Zurich, University of Zurich, Zurich, Switzerland; †Division of Infectious Diseases and Hospital Epidemiology, University Hospital Zurich, University of Zurich, Zurich, Switzerland; ‡Division of Infectious Diseases and Hospital Epidemiology, Cantonal Hospital St. Gallen, St. Gallen, Switzerland; §Department of Ophthalmology, University Hospital Basel, University Basel, Basel, Switzerland; ¶Division of Infectious Diseases and Hospital Epidemiology, University Hospital Basel, University Basel, Basel, Switzerland; and **Save Sight Institute, The University of Sydney, Sydney, Australia.

None of the authors has any financial/conflicting interests to disclose.

Reprint requests: Christian Böni, MD, Frauenklinikstrasse 24, 8091 Zurich, Switzerland; e-mail: christian.boeni@usz.ch

Assessment of Ocular Findings and Acquisition of Multimodal Imaging Findings

Patients underwent a complete ophthalmologic examination including biomicroscopy, color fundus photography with ultra-widefield photography using Optomap scanning laser ophthalmoscope (Optos, Marlborough, MA), spectral domain optical coherence tomography (OCT) including enhanced depth imaging (EDI) technique, fundus autofluorescence (FAF) imaging, fluorescein angiography/indocyanine green angiography (FA/ICGA) and, where possible, OCT angiography (OCTA). The widefield angiograms were either obtained using the Optomap system or the ultra-widefield module for the Heidelberg SPECTRALIS HRA + OCT.[8] The spectral domain OCTs and EDI-OCTs were obtained using the Heidelberg SPECTRALIS (version 1.9.10.0) as viewed with the contained Heidelberg software (Spectralis Viewing Module 6.0.9.0; Heidelberg Engineering, Heidelberg, Germany). In this study, at least 31 B-scans were obtained within a 20° × 25° rectangle centered on the macula; however, the scan pattern was adapted according to the location and the size of the lesions. Choroidal imaging was obtained using the same instrument in the EDI mode.[9] Fundus autofluorescence images were obtained in all patients using the confocal scanning laser ophthalmoscope (Heidelberg Retinal Angiograph, HRA2; Heidelberg Engineering). Optical coherence tomography angiography images were obtained using PLEX Elite 9000 swept-source OCT (Carl Zeiss Meditec, Inc., Dublin, CA) with OMAGc algorithm.[10] The scan area for this study was a 12 mm × 12 mm scan centered on the fovea and around the posterior pole to create a widefield montage image obtained with each cube consisting of 2 repeated volumes of 500 B-scans. We used the preset segmentation of the viewing software to extract the outer retina/choriocapillaris slab, which extends from 110 μm above retinal pigment epithelium (RPE) to 38 μm below RPE. In case of neovascular lesions, we used, in addition, a 3 × 3 scan centered on the lesion and we included the outer retina slab to better detect the neovascular membrane located above the RPE.

After diagnosis of ocular involvement, eye examinations were warranted every 3 to 4 months or more frequently if required, including regular multimodal imaging acquisition. Three readers (C.B., S.A.Z., and M.A.-S.) reviewed the spectrum of imaging findings in all cases. "Progressive ocular disease" was defined as occurrence of two or more new chorioretinal lesions per eye if they were not present in previous examinations and/or enlargement of previously existing choroidal lesions. The time between diagnosis of "progressive ocular disease" and "active systemic disease"

Table 1. Characteristics of Patients With Disseminated M. *chimaera* Infection and Relationships Between Ocular and Systemic Disease

	Cases			
Characteristics	2	3	4	5
Sex	Male	Male	Male	Male
Age (years)	51	64	49	61
Infection				
Time between index surgery and diagnosis	1 year 4 months	3 years 3 months	3 years 5 months	1 year 9 months
Treatment				
Tuberculostatic treatment	Clarithromycin Ethambutol Rifabutin — —	Clarithromycin Ethambutol Rifabutin Moxifloxacin Amikacin	Clarithromycin Ethambutol Rifabutin Moxifloxacin Amikacin	Clarithromycin Ethambutol Rifabutin Moxifloxacin Amikacin
Duration of tuberculostatic treatment from diagnosis to redo surgery, days	na	365 days	0 days	240 days
Redo surgery	na*	Replacement of mitral annuloplasty ring by bio mitral valve	Replacement of mechanical aortic valve by aortic root bio	Aortic root and arch replacement
Initial ocular findings	Multifocal choroiditis	Mild ocular abnormalities	Mild ocular abnormalities	Multifocal choroiditis
Outcome				
Ocular disease	Progressive choroiditis (active)	Choroidal lesions stable (inactive)	Progressive choroiditis (active)	Progressive choroiditis (active)
Follow-up of ophthalmologic monitoring (months)	1	47	51	8
Signs of systemic disease activity at diagnosis of progressive choroiditis†	Yes	na	Yes	Yes
Implications of chorioretinitis on tuberculostatic treatment	na	No	Treatment ongoing	na
Death	Yes	No	No	Yes
Healed	na	Yes	na	na
Relapse	na	No	Yes	na
Breakthrough infection	Yes	No	Yes	Yes

	Cases				
Characteristics	6	7	8	9	10
Sex	Male	Male	Male	Male	Male
Age (years)	63	64	66	50	58
Infection					
Time between index surgery and diagnosis	1 year 10 months	1 year 9 months	3 years	2 years 2 months	2 years and 1 month
Treatment					

(*continued on next page*)

Table 1. (*Continued*)

Characteristics	Cases				
	6	7	8	9	10
Tuberculostatic treatment	Clarithromycin Ethambutol Rifabutin Moxifloxacin —	Clarithromycin Ethambutol Rifabutin Amikacin —	Clarithromycin Ethambutol Rifabutin Moxifloxacin —	Clarithromycin Ethambutol Rifabutin Moxifloxacin Amikacin	Clarithromycin Ethambutol Rifabutin Moxifloxacin Amikacin
Duration of tuberculostatic treatment from diagnosis to redo surgery, days	10 days	91 days	70 days	132 days	98 days
Redo surgery	Rethoracotomy	Replacement of bio aortic valve by aortic root homograft	Replacement of bio aortic composite graft) by combined aortic valve and aorta ascendens homograft	Replacement of mitral valve annuloplasty	Replacement of aortic root and aortic arch by a homograft and bovine pericardium tube, respectively
	Debridement Graft retention	Epicardial PM implantation			Replacement of endovascular PM by epicardial PM
Initial ocular findings	Multifocal choroiditis	Multifocal choroiditis	Multifocal choroiditis	Mild ocular abnormalities	Mild ocular abnormalities
Outcome					
Ocular disease	Progressive choroiditis (active)	Choroidal lesions stable (inactive)	Progressive choroiditis (active)	Choroidal lesions stable (inactive)	Choroidal lesions stable (inactive)
Follow-up of ophthalmologic monitoring (months)	13	14	10	9	6
Signs of systemic disease activity at diagnosis of progressive choroiditis†	Yes	na	Yes	na	na
Implications of chorioretinitis on tuberculostatic treatment	na	Treatment ongoing	Treatment ongoing	Treatment ongoing	Treatment ongoing
Death	Yes	No	No	No	No
Healed	na	na	na	na	na
Relapse	na	na	na	na	na
Breakthrough infection	Yes	No	Yes	No	no

*na, not applicable.

†Systemic disease activity was defined as new positive blood cultures for mycobacteria and/or new positive mycobacterial cultures from a normally sterile site either while on tuberculostatic therapy (breakthrough infection) or in the posttreatment period (relapse).

was assessed. For classification of uveitis, criteria of the Standardization of Uveitis Nomenclature Working Group were applied.[11] Enhanced depth imaging OCT scans over the choroidal lesions were evaluated regarding full thickness/partial thickness, shape, reflectivity, internal pattern, margins, and hypertransmission. In adddition, the presence of any fluid was noted using spectral domain OCT. The en face image of the choriocapillaris was used to visualize the lesions. The OCTA image was registered to the ICGA image using the publically available ImageJ software (public domain software; National Institutes of Health, Bethesda, MD) as described previously.[12] For this purpose, the choriocapillaris OCTA image and the ICGA were registered to each other using vascular bifurcation in the superficial plexus as landmark to align the two images for accurate comparison. Changes in the choriocapillaris/inner choroid perfusion were identified. Presence of a neovascular flow/membrane in the avascular outer retina and/or sub-RPE space was evaluated.

Results

Patient Characteristics

Nine white patients (18 eyes) aged between 49 and 66 years were diagnosed with either endocarditis and/or aortic graft infection with *M. chimaera* after a cardiothoracic surgery with extracorporeal circulation.

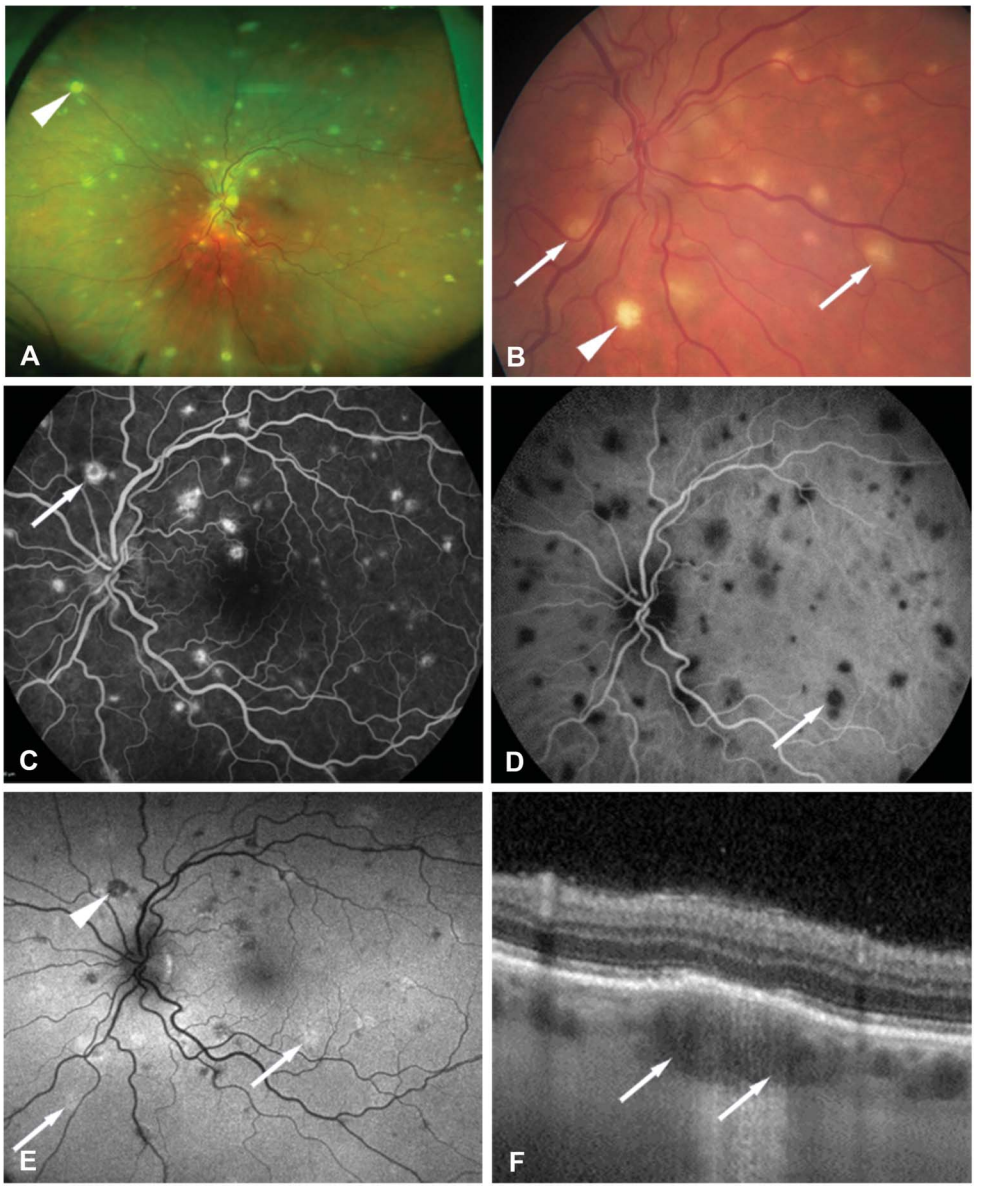

Fig. 1. Multimodal imaging of active ocular disease in disseminated *M. chimaera* infection. Ultra-widefield photography (**A**) and conventional fundus photography (**B**) show multiple roundish chorioretinal lesions. Most of the lesions show an indistinct border indicating active disease (white arrows), whereas others have well-defined borders and represent atrophic scars of formerly active lesions (arrowheads). The lesions typically show hyperfluorescence in fluorescein angiography (**C**) and hypocyanescence in indocyanine green angiography (**D**). Fundus autofluorescence (**E**) indicates both hyperautofluorescent and hypoautofluorescent areas. Enhanced depth imaging OCT (**F**) of an active chorioretinal lesion; note the full-thickness hyporeflectivity leading to focal choroidal thickening (white arrows).

All patients had a negative serology for HIV. All eyes had bilateral chorioretinal lesions. Applicable patient numbers were maintained according to previous publications.[2,7] Table 1 shows clinical characteristics of each patient including medical and surgical treatment. Mean ophthalmologic follow-up was 17.6 months. All nine patients were discovered prospectively by screening patients with known infections. At baseline, two patients reported blurred vision, whereas seven patients had no visual symptoms. During follow-up, two initially symptom-free patients described decreased vision and blurriness correlating with progressive ocular findings. Morphology of the chorioretinal lesions in these patients are described in more detail by assessing each imaging technique separately.

Multimodal Imaging Findings of Choroidal Lesions

Fundus photography. Despite the fact that all patients had chorioretinal lesions as seen using fundus

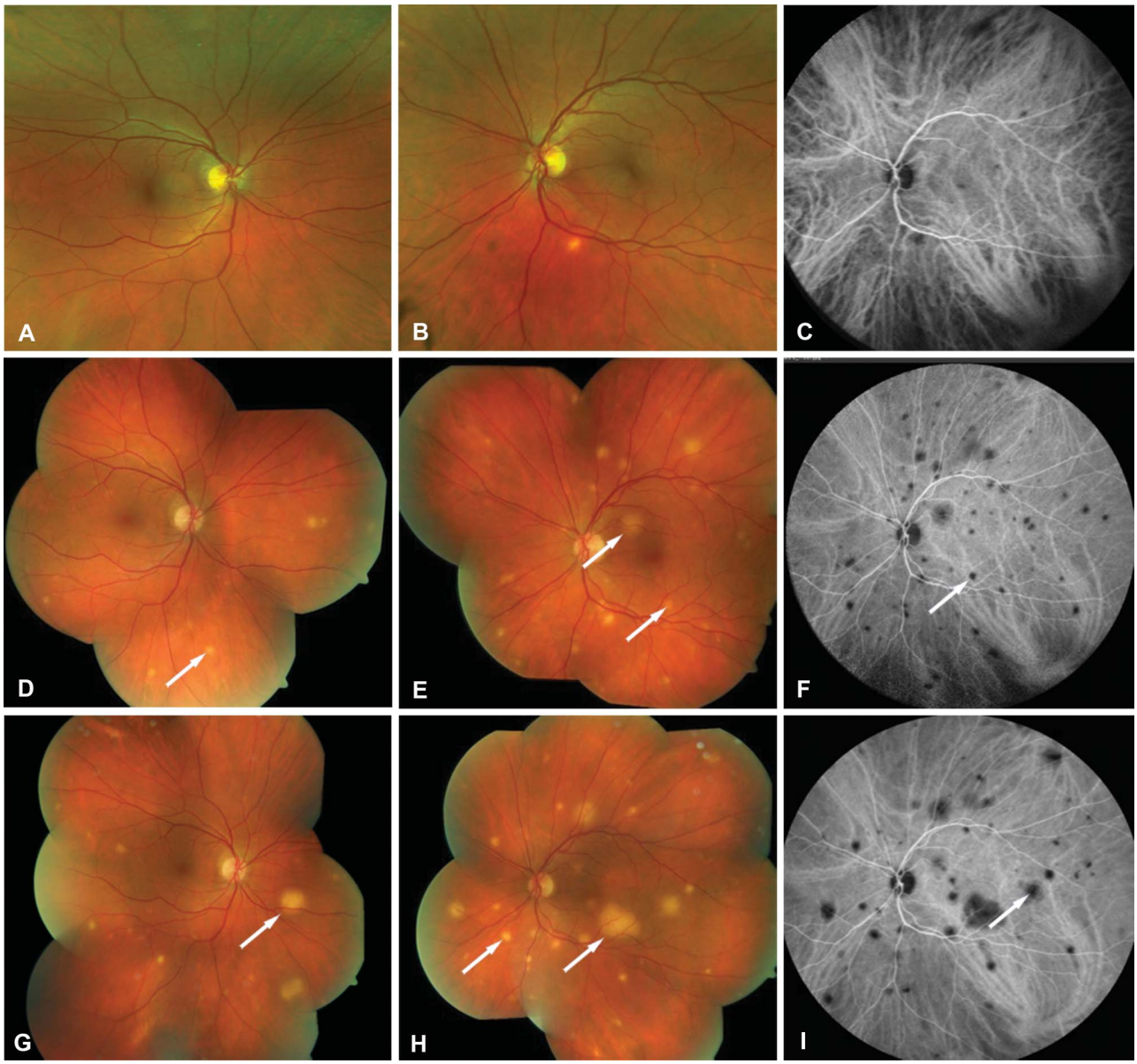

Fig. 2. Progression from inactive to active ocular disease in disseminated *M. chimaera* infection. **A–C.** Fundus photography (A, right eye; B, left eye) and indocyanine green angiography (C, left eye) of a 50-year-old patient who was diagnosed ad redo surgery. Few clinically inactive lesions were observed to be stable for over 20 months. Systemic antimycobacterial therapy was stopped after 24 months as the infection was deemed clinically inactive. **D–F.** The same patient was hospitalized 15 months later due to worsening hepatic function consistent with atypical mycobacteremia and consecutively diagnosed with a relapse based on positive mycobacterial blood cultures. In conjunction with the relapse, progression of choroidal lesions was observed. **G–I.** Five months later, despite systemic antimycobacterial treatment, more lesions became clinically evident.

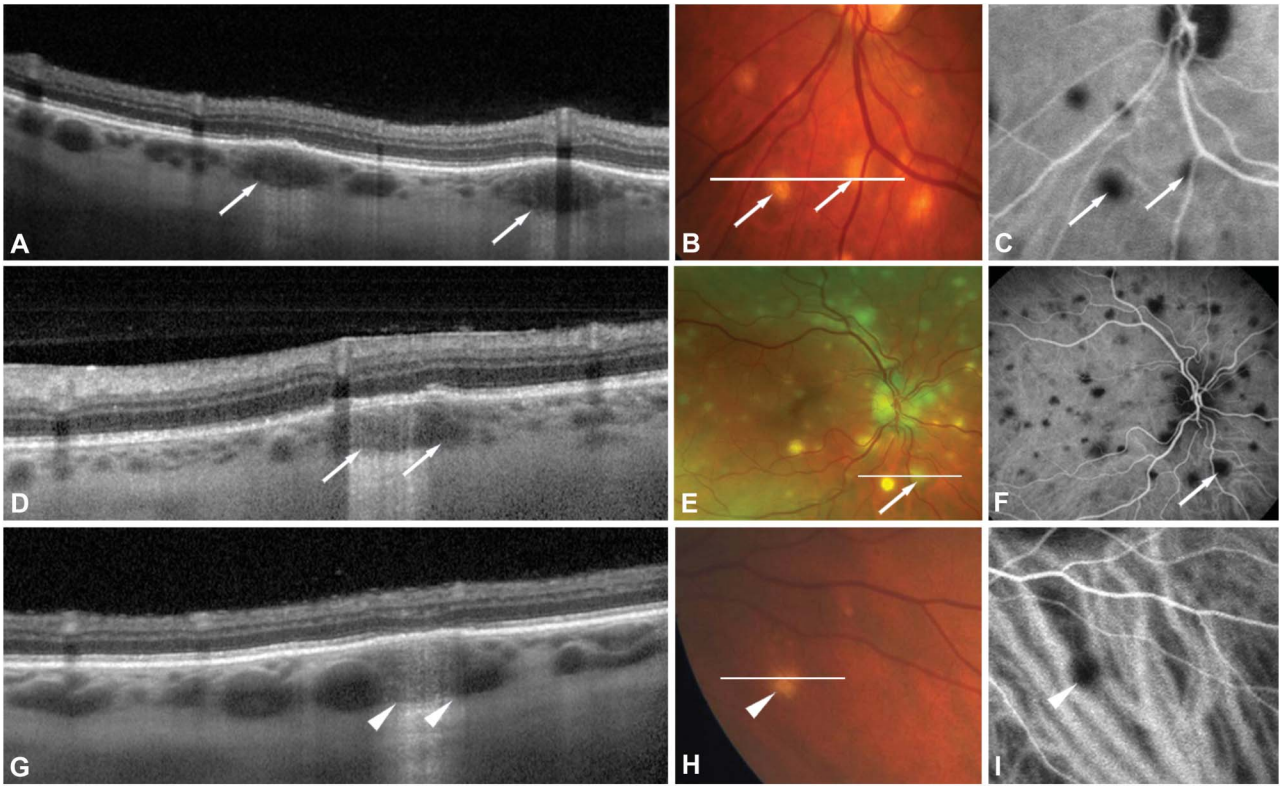

Fig. 3. Examples of choroidal lesions by EDI-OCT examination and in correlation with fundus photography (middle column) and ICGA (right column). In the active form of the disease (**A** and **D**), the borders of the lesion on EDI-OCT were found to be relatively well-defined because there usually was an intense homogenously hyporeflective area (arrows). **G.** Note the borders of this inactive lesion, which were poorly defined (arrowheads).

photography or using biomicroscopy, the extent of these lesions varied widely. At baseline, four patients had only a very few inactive (2–5/eye) choroidal lesions (mild ocular abnormalities). During follow-up, five patients (10 eyes) developed widespread lesions (progressive ocular disease). The lesions had typically a round or ovoid shape (Figures 1–4). Figure 1 shows an exemplary overview of active ocular disease in different patients using different multimodal imaging methods. Although these white-yellowish lesions were usually small (50–300 μm diameter), their size was observed to increase over weeks in active disease. An example of progressive disease over time is shown in Figure 2. Furthermore, indistinct borders on fundus photography represented a sign of activity, whereas inactivity or quiescence was related to well-defined borders of the lesions (Table 2). The largest lesion in the cohort had a diameter of 2,700 μm (Figure 5). In patients with progressive ocular disease, the number of lesions was increasing over 4 to 8 weeks and lesions were ultimately distributed diffusely over both the posterior pole and the retinal periphery. All five patients with new lesions and, therefore, active ocular disease also showed atrophic lesions suggesting formerly active lesions (Figure 1). Active and inactive lesions could be observed in close proximity in the same eye. In 3 of 5 patients with progressive ocular disease, we were able to detect a stable period with clinically inactive lesions over at least 6 months before progression to active ocular disease.

Fluorescein angiography. Active choroidal lesions in all five patients with progressive disease were initially hypofluorescent on FA, with staining in the later frames (Figures 1 and 4). However, early phase of FA showed hyperfluorescence of inactive lesions with hyperfluorescence in late phase according to a window defect. In two patients (four eyes) with progressive disease, FA also indicated a mild optic disk leakage. Otherwise, no obvious angiographic features could be observed. No eye had signs of retinal vasculitis, of capillary nonperfusion, or of cystoid macular edema.

Indocyanine green angiography. By ICGA, there were multiple hypocyanescent lesions, which were found to be hypocyanescent in both early and late frames. As compared to other means of investigation, the lesions detected on ICGA outnumbered the lesions detected on fundus photography or FA by >5 per eye in all 10 eyes with progressive disease (Figures 2 and 4). In all cases, ICGA was, therefore, superior to fundus photography for assessing occurrence of new

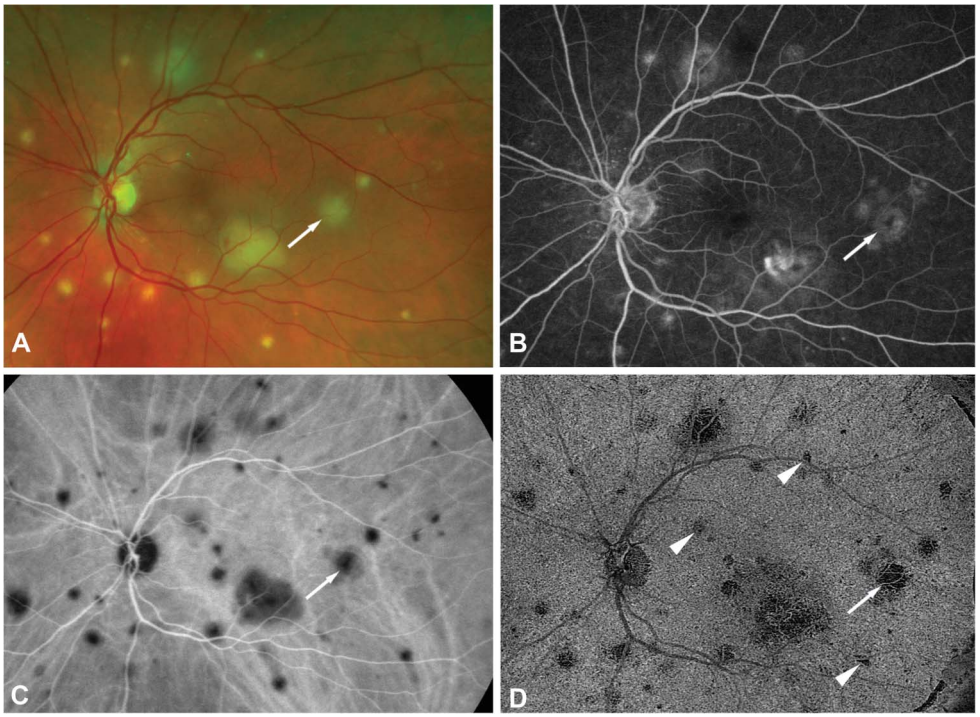

Fig. 4. Multimodal imaging and en face OCTA of chorioretinal lesions. **A.** Fundus color photography of the left eye demonstrating different-sized white-yellowish chorioretinal lesions (arrows) involving the posterior pole. **B.** Late-frame FA demonstrating few hyperfluorescent lesions throughout the posterior pole and the middle periphery. **C.** Indocyanine green angiography shows multiple hypocyanescent lesions. **D.** En face OCTA image of the choriocapillaris demonstrates multiple areas of flow reduction at the site of the lesions comparable with the ICGA. Note the outnumbered lesions compared with the FA (arrowheads).

lesions. Large active lesions showed a longer and stronger hypocyanescence in the late phase of the ICGA than inactive lesions. However, even after more than 6 months' duration, lesions still showed a faint hypocyanescence. Complete regression of the hypocyanescent areas was not observed, even in clinically quiet and sharply demarcated lesions on fundus photography, which could be explained because of atrophy of the choriocapillaris/stromal choroid.

Fundus autofluorescence. Using FAF, active chorioretinal lesions presented as hyperautofluorescent areas in all five patients with progressive disease (Figure 1). In the inactive status of the lesion, they appeared typically hypoautofluorescent. Frequently, new active hyperautofluorescent lesions could be observed close to atrophic hypoautofluorescent lesions. Lesions in the very late stages often showed a confluent hypoautofluorescence indicating confluent loss of RPE cells. Between lesions, the FAF was found to be normal without presence of pathologic hyperautofluorescence or hypoautofluorescence. However, lesions on FAF were outnumbered by lesions found on ICGA by >5 per eye in all cases with progressive disease.

Table 2. Classification of Choroidal Lesions Based on Multimodal Imaging

Imaging Modality	Active Lesion	Inactive Lesion/Lesion in Regression
Fundus photography		
Shape	Ovoid to round	Ovoid to round
Border	Indistinct	Well-defined
Size	Small (<1 disk diameter)	Small (<1 disk diameter)
Color	Yellow-white	Whitish
FA		
Early	Hypofluorescent	Hyperfluorescent
Late	Hyperfluorescent	Hyperfluorescent
ICGA	Hypofluorescent	Hypofluorescent
FAF	Hyperautofluorescent	Hypoautofluorescent
EDI-OCT		
Shape	Full-thickness, round, well-defined borders	Poorly defined margins
Internal reflectivity	Hyporeflective	Similar to the choroid
Increased transmission effect	Present	Present

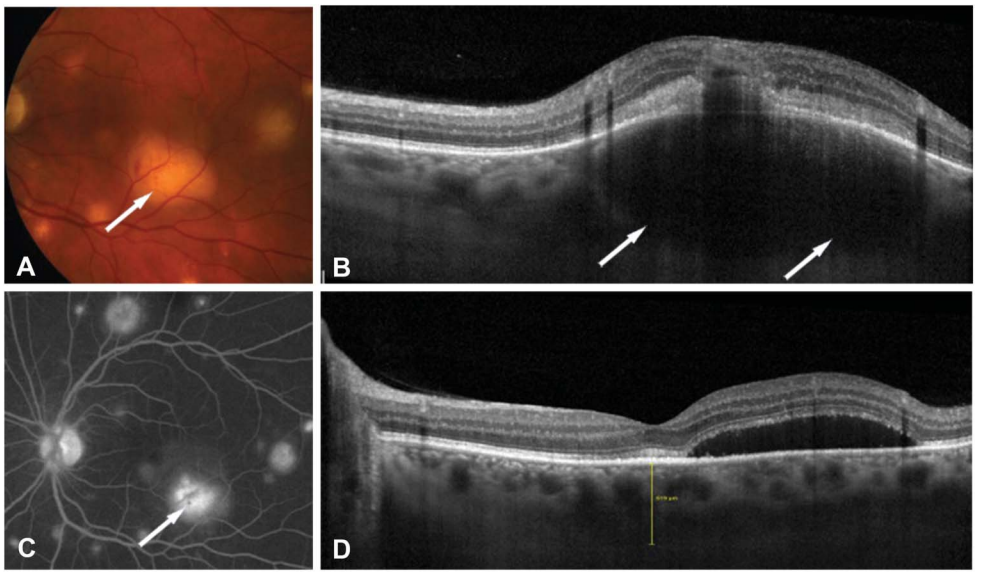

Fig. 5. Fundus photography (**A**), fluorescein angiography (**C**), and EDI-OCT (**B** and **D**) of a large, full-thickness choroidal granuloma (white arrows) with presence of active choroidal neovascularization. Note the presence of subretinal fluid and subretinal hyperreflective material. Also, the choroid is markedly thickened (white arrows).

Enhanced depth imaging ocular coherence tomography. Enhanced depth imaging OCT revealed full-thickness, round hyporeflective areas with markedly reduced choroidal vascularity in all 10 eyes with progressive disease (Figure 3). The borders of active lesions on EDI-OCT were found to be relatively well defined as there usually was an intense homogenously hyporeflective area. Inactive lesions did not always correlate with a substantial hyporeflective area. Therefore, the borders of inactive lesions were generally poorly defined (Figure 3). Full-thickness lesions were shown to affect the adjacent RPE, in such as that the latter was attenuated and irregularly shaped. Smaller, partial-thickness lesions were also present in at least some cases, but because of the smaller size, they were more difficult to verify. Hypertransmission was observed in both inactive and active lesions (Figure 3). Enhanced depth imaging OCT revealed that even alterations of the integrity of the ellipsoid zone were present over choroidal lesions (Figure 3). The size of active lesions was observed to decrease over time, whereas new lesions developed near the latter lesion. One progressively large granuloma has led to a Type 2 macular neovascularization with development of subretinal fluid above the chorioretinal lesion (Figure 5).

Optical coherence tomography angiography. Optical coherence tomography angiography was performed

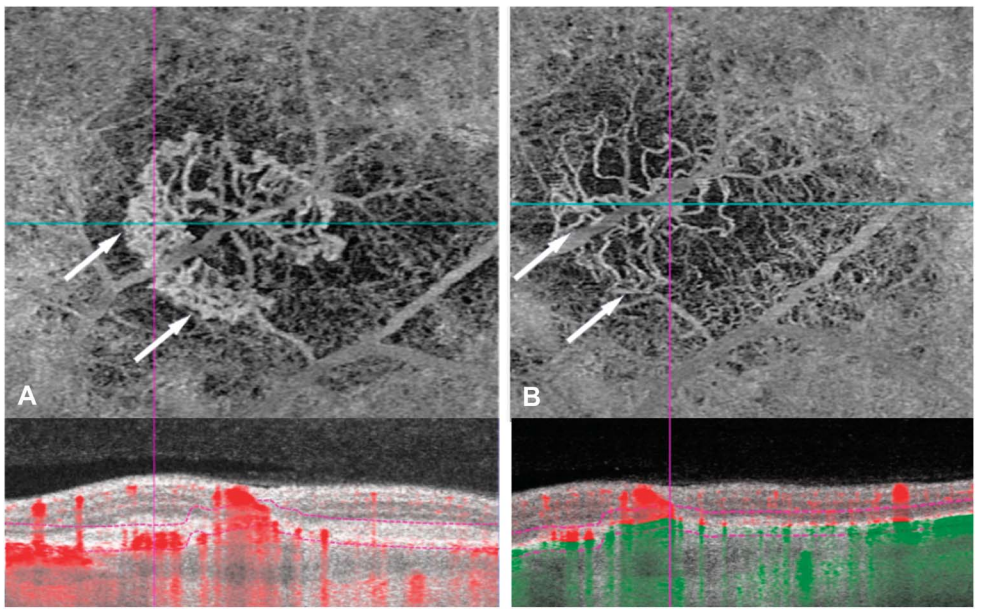

Fig. 6. Neovascular lesion before and after treatment with anti-VEGF. The left eye of this patient presented with a large chorioretinal lesion involving the posterior pole. Features of neovascularization were seen on structural OCT including subretinal hyperreflective material. In the OCTA including the en face image of the choriocapillaris and the avascular outer retina, neovascular flow with small- and medium-caliber vessels with branching of tiny vessels and arcades at the vessel termini (**A**) was observed. The right image shows the lesion 4 weeks after treatment with anti-VEGF. Note the reduced retinal thickness on the structural OCT, the decreased hyperreflective material, and the reduced area of the neovascular lesion (white arrows, **B**).

in one patient with progressive disease and in three patients with mild ocular disease. In progressive disease, the choriocapillaris/inner choroid en face OCTA image showed a flow reduction in the area that corresponded to the detected lesions on ICGA (Figure 4). Interestingly, the lesions detected by OCTA also outnumbered those found by both fundus photography and FA. The en face and cross-sectional OCTA image of a patient who reported blurry vision showed neovascular flow overlying a large chorioretinal lesion involving the posterior pole. The subretinal hyperreflective material (SHRM) detected on the structural OCT corresponded with neovascular flow presented on the en face OCTA image of the avascular outer retina/choriocapillaris (Figure 6). Morphologically, the lesions showed small- and medium-caliber vessels with branching of tiny vessel and arcades at the vessel termini. Intravitreal anti–vascular endothelial growth factor (anti-VEGF) treatment was performed, leading to marked regression of the neovascularization activity. Best-corrected visual acuity in the affected eye increased from 20/25 before therapy to 20/20 after treatment. The follow-up visit 4 weeks after anti-VEGF therapy showed a reduced retinal thickness, decreased SHRM, and reduced area and density of the neovascular membrane.

Relationship to Systemic Disease Activity

Table 1 shows relationships between ocular and systemic disease for each patient. In five of nine patients, progression of the number and size of choroidal lesions was observed despite being under systemic antimicrobial therapy. As of September 2017, 3 of these 5 patients have died because of systemic complications, potentially related to uncontrolled *M. chimaera* infection.[2,7] In four patients with progressive disease, redo surgery was either not performed or performed very late in the disease process or parts of the cardiovascular materials were retained (Cases 2, 4, 5, and 6). In one patient (Case 8), a breakthrough infection (positive blood cultures, new mycobacterial spinal lesions) was diagnosed 8 months after redo surgery and ongoing antimicrobial therapy. All 5 patients had evidence of systemic disease activity within ±6 weeks before or after the diagnosis of progressive choroiditis. In three patients, the ocular progression preceded systemic disease activity, whereas in two patients, systemic disease activity was diagnosed before ocular progression.

Discussion

Choroidal manifestation seems to be an accessible indicator of systemic disease activity in patients with disseminated *M. chimaera* infection. This study highlights the description and evolution of the chorioretinal lesions using various multimodal imaging techniques. Two particular aspects of ocular involvement were the uniform distribution and the extensive number of choroidal lesions despite antimycobacterial treatment. Monitoring disease activity in patients with disseminated *M. chimaera* disease should not be based on color fundus photography or biomicroscopy alone. Indocyanine green angiography is superior to assess the occurrence of new lesions, whereas EDI-OCT is suitable to visualize details of the choroidal lesions. Multimodal imaging is helpful for classifying lesions as active or inactive, for assessing the response to antimicrobial treatment, and for detecting early subclinical recurrences.

Enhanced depth imaging OCT allows for an assessment of structural choroidal abnormalities. In patients with *M. chimaera* infection, EDI-OCT scanning nicely indicated the size and the extent of hyporeflective lesions. The normal choroidal vascularity was markedly reduced in the affected area and we were able to demonstrate that clinically active lesions were mostly involving the full choroidal thickness extending from the back of the RPE to the choroidoscleral border. However, the lesions are generally not limited to the choroidal space, but often affect the RPE and sometimes also the outer retinal layers. These hyporeflective areas became less prominent over time and the initial homogenous hyporeflectivity gradually decreased. Histopathological investigation of these lesions in one affected subject revealed local granulomatous inflammation.[7] The presence of mycobacteria has also been hypothesized, but could not be proven, probably because of their fastidious growth.

Although EDI-OCT was suitable to monitor selected lesions, imaging with ICGA enabled a better global visualization of lesions, including central and peripheral areas. Hypocyanescent lesions on ICGA outnumbered lesions on fundus photography and on FAF, indicating that only a subset of the total choroidal lesions were either large enough or localized close enough to the RPE to be visualized by photography or FAF. These spots could result from blockage by the lesions themselves, from choroidal hypoperfusion or from displacement of vessels by space-occupying lesions. Under systemic anti-infective therapy, some lesions were observed to become less hypocyanescent but they did not completely disappear. However, this change is not proven to be treatment related and might also reflect disease evolution. Because all patients with active disease were systemically treated, the clinical course of active lesions without treatment is not clear. Our data showed that

regression of one single lesion did not necessarily correlate with the overall disease control because sometimes new lesions developed in the proximity and significantly increased in size. This might be explained by recurrent bacteremia that led to new lesions, whereas older ones were becoming smaller and atrophic after a few weeks under treatment.

The biomicroscopic presentation of the chorioretinal lesions in our series was similar to that of multifocal choroiditis related to ocular tuberculosis.[13–19] However, besides similarities there also seem to be differences between the two entities. The *M. chimaera*–related lesions were all roundish, whereas the chorioretinal lesions in tuberculosis are generally more variable in shape. Fundus imaging of ocular tuberculosis may show a more irregularly distribution compared with the picture in *M. chimaera* infection. Also, although there is a large spectrum of findings in ocular tuberculosis, none of the patients in these series presented with other findings potentially suggestive of tuberculosis such as nodular scleritis, interstitial keratitis, synechia, severe vitritis, serpiginoid choroiditis, or retinal vasculitis.[19] Choroidal lesions observed in tuberculosis usually resolve under systemic treatment over a few weeks, with residual scarring.[18,20] However, nontuberculous mycobacterium infections in and around the eye are clinically recalcitrant and may require long-term therapy and removal of biomaterials.[21]

M. chimaera–related choroiditis has not been described specifically before this current outbreak. However, other atypical mycobacteria have been reported to cause choroiditis, namely in HIV-positive patients.[22,23] Bhikoo et al have described such a case of multifocal choroiditis in an HIV patient with disseminated *M. avium* complex infection. The choroidal lesions in this subject were larger compared with the lesions in our HIV-negative *M. chimaera* patients. Multifocal choroiditis has also been reported as initial manifestation of disseminated cryptococcal infection.[24] Andreola et al[25] have described *Cryptococcus neoformans* infection and multifocal choroiditis in an HIV patient, which led to blindness. The clinical presentation in these cases was similar as the multifocal choroiditis in patients with *M. chimaera* infection.

The development of choroidal neovascularization (CNV) in the setting of an active granuloma is intriguing. Although infrequently, CNV has been reported in eyes with infectious chorioretinitis including tuberculosis, toxoplasmosis, syphilis, presumed ocular histoplasmosis syndrome, and *Bartonella henselae*.[26–32] However, in most of these cases, CNV presented not during the acute inflammatory process, but later in the setting of a chorioretinal scar. The differentiation between inflammatory-related structural alterations and neovascular lesions presenting as SHRM is by spectral domain OCT usually difficult and may result in delayed treatment. Optical coherence tomography angiography, a relatively new noninvasive technique, permits detection of vascular flow/networks relative to tissue depth and allows to distinguish vascular and avascular SHRM.[33] In our patient, neovascular flow in the subretinal space located over the granuloma could be clearly demonstrated on OCTA despite minimal leakage on FA. Optical coherence tomography angiography allowed not only to detect but also to monitor the response to treatment in disseminated *M. chimaera* infection with NV.

During prospective follow-up of these nine patients, we have observed progression in five patients and activation of previously inactive ocular disease in at least three patients so far. Because ocular disease likely reflects systemic disease activity, monitoring is highly recommended (Table 3). To provide accurate care, we herein propose baseline and follow-up eye examinations for patients at risk of *M. chimaera* infection. These recommendations were based on our observations including the aforementioned relationships between ocular and systemic progression and the fact that new lesions developed within 4 to 8 weeks. The generalizability of these recommendations is limited by the fact that this infection is overall uncommon and clinical experience is scarce. The low incidence of this infection also explains the relatively small sample size, which is a limitation of the study. The follow-up duration differs between patients and longer observation periods may show different or new insights. Interpretation of relationships between ocular and systemic findings is confounded by temporary diagnostic windows of both ophthalmologic imaging findings and systemic activity signs such as blood cultures.

In conclusion, in patients with bilateral multifocal choroiditis and a history of cardiothoracic surgery, disseminated *M. chimaera* infection should be suspected. Differentiating between active and inactive ocular disease by multimodal imaging is important because of the likely association with systemic disease activity. Thorough clinical examination, fundus photography, and EDI-OCT can detect the presence of active chorioretinal lesions, whereas FA and especially ICGA reveal the total lesion number and are better suited to detect overall disease progression. Optical coherence tomography angiography showed flow reduction at the level of choriocapillaris/inner choroid that corresponded to the lesions detected on ICGA. Whether this finding represents hypoperfusion of the choriocapillaris or displacement of the capillaries by space-occupying lesions needs to be investigated in

Table 3. Proposed Screening and Follow-up Examinations for Patients With Suspected or Confirmed *M. chimaera* Infection

Time Point	Imaging Modalities
Baseline ocular examination	Complete ophthalmic examination Visual acuity Intraocular pressure measurement Anterior and posterior segment slit-lamp examination including dilated fundus biomicroscopy Multimodal imaging testing Wide-angle fundus photography FA/ICGA (if possible using a wide-angle camera) EDI-OCT FAF OCTA (if available)
Follow-up ocular examination	
Absence of findings indicative of active disease or discontinuation of antimycobacterial therapy	Clinical follow-up visits every 2 months* Dilated fundus examination Multimodal imaging tests every 4 months*
Presence of active disease†	Clinical follow-up visits every month Dilated fundus examination Multimodal imaging tests every 2 months

*After 2 years of quiescence, the control intervals might be extended to 3 and 6 months, respectively.

†In case of suggestive findings of ocular *M. chimaera* infection, interdisciplinary management is crucial and involvement of an infectious diseases' specialist is warranted.

the future. Furthermore, analysis of en face OCTA and cross-sectional OCTA images enabled detection of neovascular flow secondary to CNV and its response to treatment with anti-VEGF.

Key words: spectral domain optical coherence tomography, fundus autofluorescence, multifocal choroiditis, choroidal tubercles, granulomatous choroiditis, nontuberculous mycobacterial infection, *Mycobacterium chimaera*, mycobacterium avium complex, cardiac surgery.

Acknowledgments

The authors thank Dr. Reinhard Rüesch and Dr. Nicole Schwizer of the Kantonsspital St. Gallen, Dr. Peter Graber of the Kantonsspital Liestal, and Dr. Frank Sachers, Private Practice Basel, for their contribution.

References

1. Sax H, Bloemberg G, Hasse B, et al. Prolonged outbreak of Mycobacterium chimaera infection after open-chest heart surgery. Clin Infect Dis 2015;61:67–75.
2. Kohler P, Kuster SP, Bloemberg G, et al. Healthcare-associated prosthetic heart valve, aortic vascular graft, and disseminated Mycobacterium chimaera infections subsequent to open heart surgery. Eur Heart J 2015;36:2745–2753.
3. Williamson D, Howden B, Stinear T. Mycobacterium chimaera spread from heating and cooling units in heart surgery. N Engl J Med 2017;376:600–602.
4. Chand M, Lamagni T, Kranzer K, et al. Insidious risk of severe Mycobacterium chimaera infection in cardiac surgery patients. Clin Infect Dis 2017;64:335–342.
5. Svensson E, Jensen, ET, Rasmussen EM, et al. Mycobacterium chimaera in heater-cooler units in Denmark related to isolates from the United States and United Kingdom. Emerg Infect Dis 2017;23:507–509.
6. Lyman MM, Grigg C, Kinsey CB, et al. Invasive nontuberculous mycobacterial infections among cardiothoracic surgical patients exposed to heater-cooler devices1. Emerg Infect Dis 2017;23:796–805.
7. Zweifel SA, Mihic-Probst D, Curcio CA, et al. Clinical and histopathologic ocular findings in disseminated Mycobacterium chimaera infection after cardiothoracic surgery. Ophthalmology 2017;124:178–188.
8. Witmer MT, Parlitsis G, Patel S, Kiss S. Comparison of ultra-widefield fluorescein angiography with the Heidelberg Spectralis((R)) noncontact ultra-widefield module versus the Optos ((R)) Optomap((R)). Clin Ophthalmol 2013;7:389–394.
9. Spaide RF, Koizumi H, Pozzoni MC. Enhanced depth imaging spectral-domain optical coherence tomography. Am J Ophthalmol 2008;146:496–500.
10. Huang Y, Zhang Q, Thorell MR, et al. Swept-source OCT angiography of the retinal vasculature using intensity differentiation-based optical microangiography algorithms. Ophthalmic Surg Lasers Imaging Retina 2014;45:382–389.
11. Jabs DA, Nussenblatt RB, Rosenbaum JT. Standardization of uveitis nomenclature for reporting clinical data. Results of the First International Workshop. Am J Ophthalmol 2005;140: 509–516.
12. Schneider CA, Rasband WS, Eliceiri KW. NIH Image to ImageJ: 25 years of image analysis. Nat Methods 2012;9: 671–675.
13. Agrawal R, Gupta B, González-López JJ, et al. Spectrum of Choroidal Involvement in Presumed Ocular Tuberculosis: Report from a Population with Low Endemic Setting for Tuberculosis. Ocul Immunol Inflamm 2017;25:97–104.
14. Mehta S. Ocular lesions in acute disseminated tuberculosis. Ocul Immunol Inflamm 2004;12:311–315.
15. Moorthy RS, Valluri S, Rao NA. Nontuberculous mycobacterial ocular and adnexal infections. Surv Ophthalmol 2012;57: 202–235.
16. Nazari Khanamiri H, Rao NA. Serpiginous choroiditis and infectious multifocal serpiginoid choroiditis. Surv Ophthalmol 2013;58:203–232.
17. Abu El-Asrar AM, Abouammoh M, Al-Mezaine HS. Tuberculous uveitis. Int Ophthalmol Clin 2010;50:19–39.
18. Gupta V, Gupta A, Rao NA. Intraocular tuberculosis—an update. Surv Ophthalmol 2007;52:561–587.

19. Gupta V, Shoughy SS, Mahajan S, et al. Clinics of ocular tuberculosis. Ocul Immunol Inflamm 2015;23:14–24.
20. Shakarchi FI. Ocular tuberculosis: current perspectives. Clin Ophthalmol 2015;9:2223–2227.
21. Girgis DO, Karp CL, Miller D. Ocular infections caused by non-tuberculous mycobacteria: update on epidemiology and management. Clin Exp Ophthalmol 2012;40:467–475.
22. Bhikoo R, Bevan R, Sims J. Multifocal choroiditis with panuveitis in a patient with disseminated Mycobacterium avium complex. Retin Cases Brief Rep 2013;7:155–157.
23. Zamir E, Hudson H, Ober RR, et al. Massive mycobacterial choroiditis during highly active antiretroviral therapy: another immune-recovery uveitis? Ophthalmology 2002;109:2144–2148.
24. Babu K, Murthy KR, Rajagopalan N. Primary bilateral multifocal choroiditis as an initial manifestation of disseminated cryptococcosis in a HIV-positive patient. Ocul Immunol Inflamm 2008;16:191–193.
25. Andreola C, Ribeiro MP, de Carli CR, et al. Multifocal choroiditis in disseminated Cryptococcus neoformans infection. Am J Ophthalmol 2006;142:346–348.
26. Balaskas K, Spencer S, D'Souza Y. Peripapillary choroidal neovascularisation in the context of ocular syphilis is sensitive to combination antibiotic and corticosteroid treatment. Int Ophthalmol 2013;33:159–162.
27. Bansal R, Bansal P, Gupta A, et al. Diagnostic Challenges in Inflammatory Choroidal Neovascular Membranes. Ocul Immunol Inflamm 2017;25:554–562.
28. Lodhi SA, Saifuddin K, Devulapally S. Inflammatory choroidal neovascular membrane after healed tuberculous choroidal granuloma. GMS Ophthalmol Cases 2017;7:Doc06.
29. Latanza L, Viscogliosi F, Solimeo A, et al. Choroidal neovascularisation as an unusual ophthalmic manifestation of cat-scratch disease in an 8-year-old girl. Int Ophthalmol 2015; 35:709–716.
30. Petrou P, Georgalas I, Markomichelakis N, et al. Resolution of vitreomacular traction following intravitreal ranibizumab in cases of ocular toxoplasmosis with choroidal neovascularization. Ther Clin Risk Manag 2013;9:391–394.
31. Hegde S, Relhan N, Pathengay A, et al. Coexisting choroidal neovascularization and active retinochoroiditis-an uncommon presentation of ocular toxoplasmosis. J Ophthalmic Inflamm Infect 2015;5:22.
32. Halperin LS, Lewis H, Blumenkranz MS, et al. Choroidal neovascular membrane and other chorioretinal complications of acquired syphilis. Am J Ophthalmol 1989;108:554–562.
33. Dansingani KK, Tan AC, Gilani F, et al. Subretinal hyperreflective material imaged with optical coherence tomography angiography. Am J Ophthalmol 2016;169:235–248.